
Differentiable Optimization of Similarity Scores Between Models and Brains

Nathan Cloos
MIT
nacloos@mit.edu

Moufan Li
NYU
moufan.li@nyu.edu

Markus Siegel
HIH Tübingen
markus.siegel@uni-tuebingen.de

Scott L. Brincat
MIT
sbrincat@mit.edu

Earl K. Miller
MIT
ekmiller@mit.edu

Guangyu Robert Yang
MIT
yanggr@mit.edu

Christopher J. Cueva
MIT
ccueva@gmail.com

Abstract

What metrics should guide the development of more realistic models of the brain? One proposal is to quantify the similarity between models and brains using methods such as linear regression, Centered Kernel Alignment (CKA), and angular Procrustes distance. To better understand the limitations of these similarity measures we analyze neural activity recorded in five experiments on nonhuman primates, and optimize synthetic datasets to become more similar to these neural recordings. How similar can these synthetic datasets be to neural activity while failing to encode task relevant variables? We find that some measures like linear regression and CKA, differ from angular Procrustes, and yield high similarity scores even when task relevant variables cannot be linearly decoded from the synthetic datasets. Synthetic datasets optimized to maximize similarity scores initially learn the first principal component of the target dataset, but angular Procrustes captures higher variance dimensions much earlier than methods like linear regression and CKA. We show in both theory and simulations how these scores change when different principal components are perturbed. And finally, we jointly optimize multiple similarity scores to find their allowed ranges, and show that a high angular Procrustes similarity, for example, implies a high CKA score, but not the converse.

Project page: <https://diffscore.github.io>

Code: <https://github.com/diffscore/diffscore>

Similarity package: <https://github.com/diffscore/similarity-repository>

1 Introduction

Natural intelligence entails the interactions between many systems - such as different sensory, memory, and motor systems. Therefore, ultimately, many of the open questions in systems neuroscience will require models that bridge these systems. However, there are many challenges as we work towards these multi-system models of the brain. We need guidance to search through this huge design space of potential models. It would be helpful to have metrics that allow us to extract general principles that are applicable across many models, or alternatively, highlight the power of heterogeneity, and shine a spotlight on combinations of tasks, datasets, and models that are not currently well explained.

Preprint. Under review.

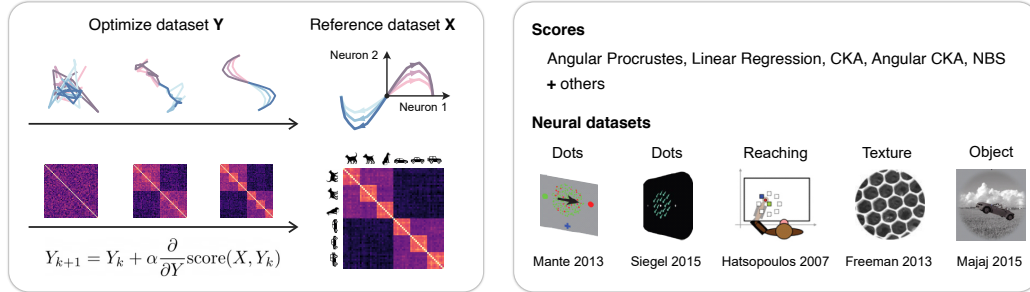


Figure 1: (a) To better understand the properties of similarity measures we optimize synthetic datasets to become more similar to a reference dataset, for example, neural recordings. (b) We analyzed similarity scores between artificial datasets and electrode recordings from five experiments on nonhuman primates spanning a diverse range of behaviors and brain regions.

Similarity measures have become a cornerstone in evaluating representational alignment across different models [Kornblith et al., 2019], different biological systems [Kriegeskorte et al., 2008], and across both artificial and biological systems. Researchers have employed diverse methods to compare model representations with, for example, brain activity, aiming to identify models that exhibit brain-like representations [Yamins et al., 2014, Sussillo et al., 2015, Schrimpf et al., 2018, Nayebi et al., 2018]. However, while these measures are actively used and provide an efficient way to compare structure across complex systems, it is not clear that they adequately represent the computational properties of interest, and there is a need to better understand their limitations. The field lacks clear guidelines for selecting the most appropriate measure for a given context.

In this work we study several popular methods that have been proposed to quantify the similarity between models and neural data, in particular, linear regression [Yamins et al., 2014, Schrimpf et al., 2018], Centered Kernel Alignment (CKA) [Kornblith et al., 2019], and angular Procrustes distance [Williams et al., 2021, Ding et al., 2021]. See appendix B.1 for a brief overview. We analyzed neural data from studies on nonhuman primates (Figure 1) and compared the neural responses to task-optimized recurrent neural networks (RNNs), or synthetic datasets, with different similarity scores. In order to study what drives high similarity scores we directly optimize the synthetic datasets to maximize their similarity to the neural datasets as assessed by different methods, for example, linear regression, CKA, or angular Procrustes distance.

Comparing similarity scores across studies is challenging, primarily due to variability in naming and implementation conventions. As part of our contribution to the research community we have created, and are continuing to develop, a *Python package* that benchmarks and standardizes similarity measures.

Disagreement between similarity measures. An example application of similarity measures is to quantify how brain-like models are. However, when we compare task-optimized RNNs to two neural datasets, as shown in Figure 2, we find that different similarity measures do not agree about which models are more similar to the data, or even about whether the models are more or less similar than two baseline scores that compare modified versions of the neural data to the original neural data. Are most of the models generally performing well or not, i.e. achieving model-data similarities above one or both of these baseline scores? Different measures give different answers. These similarity measures lack consistency and do not present a consensus interpretation. This is not an irrelevant exercise as all of these similarity measures have been used in the literature to compare models to neural data.

2 Related Work

Reviews. Recent reviews by Sucholutsky et al. [2023] and Klabunde et al. [2023] provide comprehensive overviews of representational similarity measures and their theoretical properties. While these reviews highlight the diversity of available metrics, they offer limited practical guidance on metric selection.

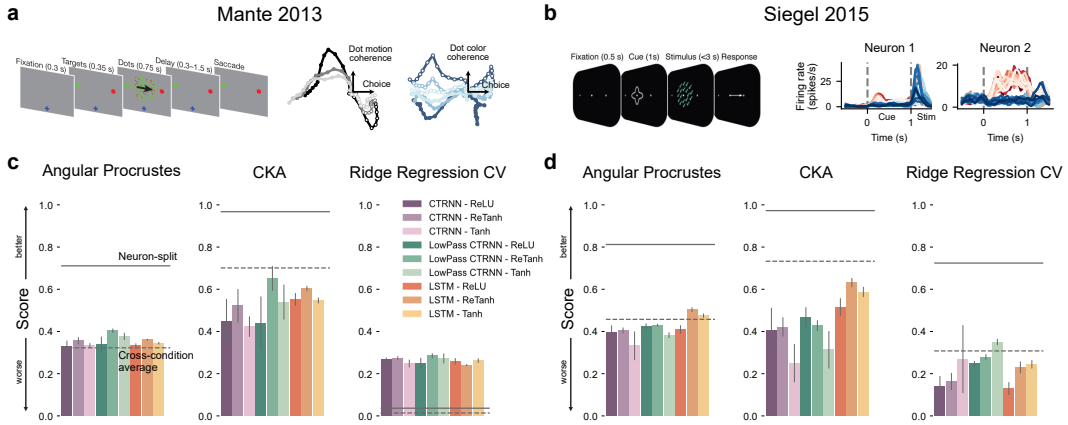


Figure 2: Different similarity measures are not consistent when comparing task-optimized recurrent neural networks to neural datasets. We consider two neural datasets from prefrontal cortex (PFC) [Mante et al., 2013] (a) and Frontal Eye Field (FEF) [Siegel et al., 2015] (b) in monkeys performing an experimental task that required the animal to attend to either color or motion information while ignoring the non-cued feature of the stimuli. On each trial, a field of colored moving dots is shown. Monkeys are given a cue at the beginning of the trial to determine whether the dots in the stimulus are moving left vs right, or are red vs green. The monkey reported its choice with a saccade to one of two visual targets. In both datasets, we analyzed neural activity taken when the dot stimulus was presented. In panel a neural activity is visualized in a low-dimensional space capturing task-relevant dynamics using the targeted dimensionality reduction method from Mante et al. 2013. Each curve shows the average neural activity for a different experimental condition. See Mante et al. 2013 for a detailed description of the analysis. This visualization highlights features of the data but the similarity scores were computed using the firing rates from the electrode recordings before any dimensionality reduction. In panel b neural firing rates for two example neurons are shown with the colors denoting average activity for different experimental conditions. (c, d) RNNs with three different architectures, CTRNN, LowPassCTRNN, LSTM and three different nonlinearities, ReLU, ReTanh, Tanh are compared to neural datasets. The Neuron-split baseline score was obtained by dividing the neurons from a single dataset into disjoint sets and then comparing. If the model-data scores are equal to the neuron-split scores this indicates that model activity is indistinguishable from the neural activity of other recorded neurons. The Condition-average baseline score was obtained by averaging the neural activity along the trial and condition dimensions and comparing it to the original dataset. Each neuron in this condition-averaged dataset still has a unique time-varying firing rate. This strong baseline shows the similarity to the original data that one can obtain by only keeping the condition-independent neural dynamics. **The different similarity measures do not agree on the relative rankings of the models, or on a more global scale, how similar the models are relative to the two baseline scores.**

Our work addresses this gap by proposing a general framework for comparing similarity measures on experimental neural datasets. By directly optimizing synthetic datasets to maximize their similarity to neural recordings, we can systematically investigate how different metrics prioritize various aspects of the data, such as specific principal components or task-relevant information.

Mathematical properties. This work builds upon several important theoretical and empirical contributions. Kornblith et al. [2019] discussed the invariance properties of similarity measures and their implications for comparing neural representations. Williams et al. [2021] advocated for similarity measures that satisfy the axioms of a metric distance. Harvey et al. [2023] established a duality between Normalized Bures Similarity (NBS) and Procrustes distance, shedding light on their mathematical relationship to CKA. We leverage these theoretical insights to provide a deeper interpretation of our empirical findings.

Comparison with functional measures. Our approach shares similarities with the work of Ding et al. [2021], who evaluated metrics based on their correlation with functional behavioral measures. They analyzed a collection of trained models and observed how variations in the models, such as the removal of principal components, impacted both the similarity scores and the performance on

task-specific probes. They identified that CKA exhibited sensitivity primarily to the top principal components, while orthogonal Procrustes demonstrated more robust performance.

However, our approach differs significantly in how we construct a diverse set of datasets with varying behavioral characteristics. Instead of relying on pre-trained models, we begin with unstructured noise and directly optimize it to maximize similarity to neural recordings. This allows us to address questions such as whether high similarity scores can be achieved without encoding task-relevant variables. Our optimization-based approach reveals how different similarity measures guide the emergence of task-relevant information within the synthetic datasets, offering a dynamic perspective on their properties.

In contrast to the majority of previous work, our method is model-agnostic, focusing on the properties of similarity measures themselves rather than specific model architectures. We demonstrate the generalizability of our findings by applying our framework to multiple neural datasets, revealing consistent patterns in how different metrics prioritize data features. Interestingly, we find that the optimization dynamics observed with neural data are closely predicted when using Gaussian datasets with matched variance distributions. This suggests that our insights extend beyond the specifics of individual neural datasets and reflect fundamental properties of the similarity measures themselves.

3 Method

To evaluate the similarity of representations between two systems, we extract feature representations such as activity in a brain area or model layer in response to stimuli. Our objective is to quantify the alignment between these representations using a similarity score. Assume two datasets X and Y represent these features with dimensions (sample, feature) and mean-centered columns. Datasets with temporal dynamics are reshaped from (time, sample, feature) to (time*sample, feature). We define a scoring function $\text{score}(X, Y)$ as a measure that increases with similarity, achieving a maximum of 1 when $X = Y$.

We show results for the following three common similarity measures (see appendix B.1 for details):

- **Linear Regression** finds the best linear mapping B that predicts a reference dataset X from a dataset Y [Yamins et al., 2014, Schrimpf et al., 2018]. We measure the goodness of fit using R^2 and use ridge regularization with parameter $\lambda = 100$ as well as 5-fold cross-validation that tests generalization across different experimental conditions.

$$R_{LR}^2 = 1 - \frac{\min_B \|X - YB\|_F^2 + \lambda \|B\|_F}{\|X\|_F^2}$$

- **Centered Kernel Alignment (CKA)** measures the correlation between the kernels of two datasets X and Y [Kornblith et al., 2019]. We consider here linear CKA where the kernels are XX^T and YY^T .

$$\text{CKA}(X, Y) = \frac{\langle \text{vec}(XX^T), \text{vec}(YY^T) \rangle}{\|XX^T\|_F \|YY^T\|_F}$$

We also consider the angular version of CKA [Williams et al., 2021, Lange et al., 2022].

- **Angular Procrustes** finds the optimal orthogonal linear alignment between X and Y to maximize their correlation [Williams et al., 2021, Ding et al., 2021].

$$\max_{Q \in \mathcal{O}} \frac{\langle X, QY \rangle}{\|X\|_F \|Y\|_F}$$

where \mathcal{O} is the group of orthogonal linear transformations. Williams et al. [2021] proposed taking the arccosine to satisfy the axioms of a distance metric. Here we rescale the angular Procrustes distance to obtain a scoring measure between 0 and 1, where 1 is perfect similarity.

4 Results

4.1 High similarity scores do not guarantee encoding of task relevant variables

Question. We start by asking if synthetic datasets with high similarity scores relative to the neural data, encode task relevant variables, for example, the stimulus features or the response of the monkey,

in the same way as the neural data. More specifically, is it possible for the synthetic datasets to have a high similarity score while failing to encode task relevant variables?

Problem with CKA and linear regression. Surprisingly we find that for linear regression and CKA the answer is yes, a high similarity score does not necessarily mean the synthetic datasets encode task relevant variables like the neural data. Figures 3a and 3b show the decode accuracy of a linear classifier trained to decode task relevant variables (cross-validated across different conditions) as the similarity score increases. Before optimization, the synthetic datasets initially consisted of Gaussian noise and the decode accuracy was near the baseline chance level of 0.5 as expected for the binary classifier used in this analysis.

Consider the synthetic data optimized towards the Siegel 2015 neural recordings using CKA similarity (second row and column in Figure 3). When the synthetic dataset has a high similarity score of 0.9 the decode accuracy for all the task variables is still less than that found in the neural activity (horizontal dashed lines). This is in contrast to the case where synthetic data is optimized to maximize angular Procrustes similarity (first column) and a similarity score of near 0.9 yields a dataset that encodes task variables to the same degree as the neural recordings. Note that both CKA and angular Procrustes have the same similarity scale ranging between 0 and 1 (perfect similarity). See appendix B.1 for more details.

As another example, consider the decode accuracy for the color of the stimulus that was shown in the experiments (green curves). For linear regression and CKA the similarity score can be high even when the data does not encode this task variable at the level found in the neural activity, suggesting there is a mismatch between the datasets with a high similarity score and features of the neural activity. In contrast, for the angular Procrustes distance the synthetic datasets that have a high similarity score relative to the neural activity also encode the task relevant variables.

How high should a good score be? As a final more optimistic note, for all the similarity measures, we can see a general trend that optimizing the synthetic data towards higher similarity eventually leads the data to encode task relevant variables above the baseline chance level of 0.5 accuracy. One perspective on this decoding analysis is that it gives a window into what is a *high* similarity score. If a high score is one where the data is encoding task relevant variables then these similarity numbers will need to be *interpreted differently* based on the similarity measure.

High variability in the condition average baseline across metrics. A specific number for the similarity score, 0.9 for example, can have different interpretations depending on the measure that is used, as we have seen in the examples above contrasting CKA and angular Procrustes. Conversely if two models or datasets are compared then this comparison may result in different scores depending on the similarity measure. Prior work has used the *condition average baseline* as a reference score for benchmarking models against neural data [Cloos et al., 2022]. The condition average baseline is obtained by averaging each neuron’s activity across trials from all experimental conditions, while still allowing each neuron to have its own unique time-varying firing rate, and then comparing this condition-averaged dataset to the original neural data. This baseline shows the similarity one can obtain by discarding the condition specific activity to keep only the condition independent dynamics of the neural activity. The condition average baseline is shown in Figures 3a and 3b as vertical dashed lines. For a single dataset, we are always comparing the same two quantities to obtain the condition average baseline but the scores are quite different depending on the similarity measure. For the angular Procrustes measure, as opposed to the linear regression similarity measure, this baseline score is closer to the point where task relevant information starts to be encoded.

4.2 Optimization dynamics of similarity scores

4.2.1 Low-dimensional synthetic datasets

Question. How much of the neural data must be captured by a synthetic dataset or model before the decode accuracy reaches the level seen in the neural dataset itself? One perspective on this question is to decode the task variables from neural data after projecting onto principal components 1 through N , where principal component 1 captures the most variance. In order to capture all the information about the task variables, at least several principal components must be included in the decode as shown in Figures 3c and 3d. This motivates the following hypothesis.

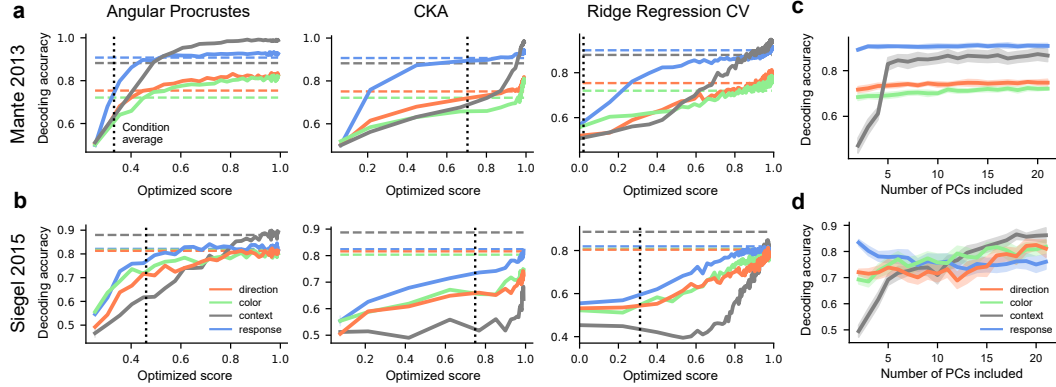


Figure 3: *(a, b)* **Decode accuracy for experimental variables versus similarity scores.** Decode is from synthetic data optimized towards greater similarity with the neural data from *(a)* Mante et al. [2013] and *(b)* Siegel et al. [2015]. Horizontal dashed lines indicate the decode accuracy from the neural data. *(c, d)* Decode accuracy from neural data versus number of principal components included in the decode. Decode uses data from *(c)* prefrontal cortex from Mante et al. 2013 and *(d)* FEF from Siegel et al. 2015.

Hypothesis. Perhaps the reason that linear regression and CKA similarity scores can be so high while the synthetic data fails to encode task variables is because these similarity measures preferentially rely on the top few principal components.

We explore this hypothesis in the following set of analyses with a synthetic dataset based on the neural recordings from Mante et al. 2013.

Figure 4a shows the reference dataset (compare to Figure 2a). We can think of this reference dataset as a low-dimensional neural trajectory summarizing the population activity of many neurons, or alternatively, as the firing rates of two neurons over time (shown here encoding the two task variables of choice and dot motion coherence), recorded during six different experimental conditions, with the color in Figure 4a denoting the condition.

Figure 4b shows the transformation of an initially random Gaussian noise dataset as it is optimized to maximize either the angular Procrustes or CKA similarity score with respect to the reference dataset. The score increases from an initial value near 0 to a maximum near 1 as optimization progresses, with the insets at the top of the figure showing the optimized noise dataset at various points during this procedure. The yellow curve shows how well the optimized dataset captures the first principal component of the reference dataset, as quantified by R^2 , throughout optimization (see appendix B.2 for details). Notice that the second principal component, shown in purple, is only captured at a *much higher* optimization score for CKA versus angular Procrustes.

Figure 4c shows the same results when a synthetic Gaussian noise dataset is optimized towards the reference dataset using either linear regression similarity or angular CKA similarity [Williams et al., 2021].

Dependence on the variance distribution. The optimization dynamics not only depend on the similarity measure but also on the variance distribution of the reference dataset. Figure 4d shows four reference datasets with the same variance along the first principal component but decreasing variance along the second. If both dimensions have approximately equal variance then angular Procrustes, CKA, and linear regression will learn both dimensions similarly during optimization as shown by the white curve in Figure 4e. The curves are colored to indicate the fraction of variance the second principal component has relative to the first, so 1 indicates both principal components have the same variance. As the asymmetry between the principal components grows, the optimization to maximize angular Procrustes similarity still prioritizes the lower variance principal component (first column, second row), while CKA and linear regression do not capture the second principal component of the reference dataset until much later during optimization.

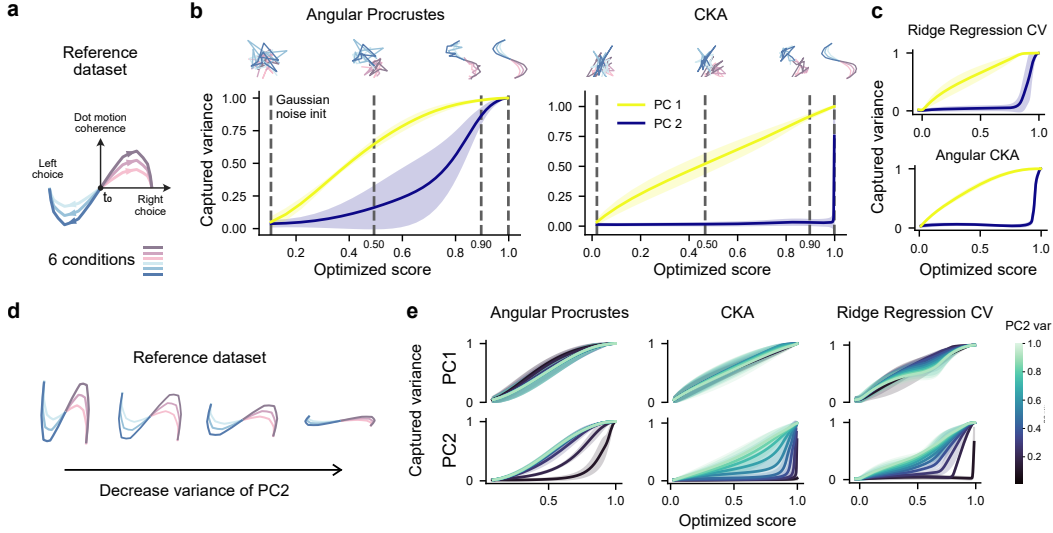


Figure 4: **Different similarity measures differentially prioritize learning principal components of the data.** (a) Reference dataset used as a target during optimization. (b, c) Initial Gaussian random noise data is updated to maximize similarity with the reference dataset, as quantified by one of the similarity measures. The transformation of the random noise dataset is shown at the top of panel b. The first principal component of the reference dataset is increasingly well captured by the optimized data as the similarity scores increase (yellow curves). **The second, lower variance, component is also learned when maximizing the angular Procrustes similarity but is only captured at high similarity scores when maximizing linear regression, CKA, and angular CKA similarity.** (d) Four reference datasets with decreasing variance along the second principal component. (e) Similarity measures capture both principal components when their variance is approximately equal. However, when the variance differs, CKA and linear regression have a much more pronounced preference for learning the high variance component as opposed to angular Procrustes which causes the optimized dataset to also capture the low variance dimension (curves colored according to asymmetry of variance distribution).

4.2.2 Neural datasets

The optimization dynamics revealed in Figure 4a for a two-dimensional dataset also holds on real neural datasets (A.1). We now consider various neural datasets as the reference dataset for the optimization procedure. Figure 5a shows the optimization dynamics when a random noise Gaussian dataset is optimized towards the Siegel et al. 2015 dataset by maximizing angular Procrustes similarity (top) or CKA similarity (bottom). Each curve shows how the optimized dataset captures a single principal component of the reference dataset during the course of optimization. Similar to the results in Figure 4, optimizing for angular Procrustes similarity captures more of the lower variance components in the data for a given similarity score.

A convenient way of summarizing these curves is to note the similarity score required to capture a given principal component above some threshold, defined here (and shown in Figure 5a) as the centerpoint between the maximum and initial R^2 value for a given principal component. Figure 5b shows the score required to reach the principal component threshold for the different principal components in the Mante et al. 2013 dataset. Figures 5c and 5d show the same curves when the reference datasets are now the electrode recordings from Siegel et al. 2015 and Majaj et al. 2015.

Angular CKA. Williams et al. [2021] proposed to take the arccosine of CKA to obtain a measure that satisfies the axioms of a distance metric. Figures 5b, 5c, and 5d additionally show that the metric version of CKA (referred to as angular CKA) improves its sensitivity to lower variance components.

Neural curves predicted by matched Gaussians. Surprisingly, the optimization dynamics shown in these figures is well matched when the reference neural dataset is replaced by a new reference dataset that consists of random Gaussian numbers with variances for each principal component matched to

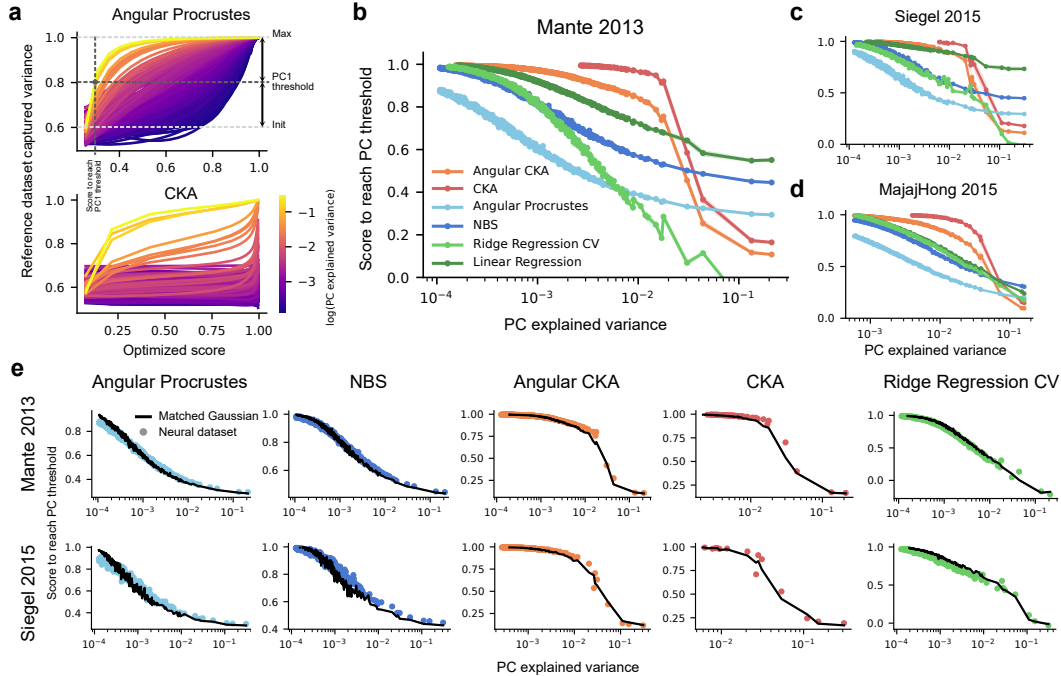


Figure 5: (a) A randomly initialized synthetic dataset is updated to maximize the similarity with a neural dataset, taken here to be the FEF dataset from [Siegel et al., 2015]. The principal components (PCs) of this reference dataset are captured by the optimized dataset at different similarity scores, which in subsequent figures we call the score to reach the PC threshold. (b) The score to reach the PC threshold for the [Mante et al., 2013] dataset is shown as a function of the variance explained by each PC. The highest variance PC is learned first during optimization at the lowest similarity score (bottom right of figure). A vertical slice through the figure shows the similarity score required to capture a specific PC. For example, to capture the PC at 10^{-2} requires a much lower similarity score when maximizing angular Procrustes versus CKA (light blue curve is below the red curve). (c, d) The reference dataset used as a target during optimization is the neural activity from [Siegel et al., 2015] FEF (panel c) and [Majaj et al., 2015] (panel d). (e) The neural data points are the same as in panels c and d (colored dots). The similarity scores at which PCs of this neural activity are learned, is well predicted by replacing neural activity with random Gaussian datasets that have a matching distribution of variances for each PC (black curves).

the neural data (Figure 5e). The variance distribution of the reference dataset strongly determines when each principal component is captured during optimization.

4.3 Theoretical analysis of CKA and NBS

Ding et al. [2021] briefly noted in their discussions that in the simplified case where two datasets have the same eigenvectors, CKA reduces to products of squared singular values of each dataset, whereas Procrustes distance doesn't square the singular values. Here we provide a more formal way to derive this result, leveraging a duality relationship discovered by Harvey et al. [2023].

Duality of Bures and shape distances. Harvey et al. [2023] showed that angular Procrustes is related to another measure, Normalized Bures Similarity (NBS) [Tang et al., 2020], by just taking the arccosine. Similar to angular CKA, we find that the arccosine increases sensitivity to lower variance components (Figures 5b, 5c, and 5d). This can be understood by the nonlinear mapping of arccosine that expands values close to one.

To understand the increased sensitivity to low variance principal components of NBS compared to CKA (dark blue and red curves in Figures 5b, 5c, and 5d), we analyze their matrix norm formulation. As shown in Harvey et al. [2023], CKA and NBS can be formulated as follow (see appendix B.1 for

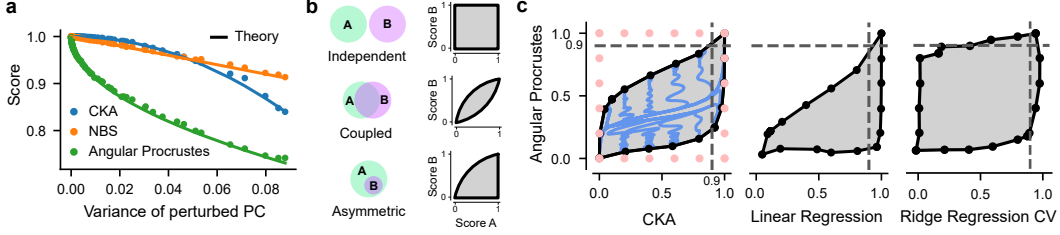


Figure 6: (a) The similarity score between a synthetic dataset and a modified version of the same dataset when a single principal component is perturbed. For all similarity measures, when small variance components are perturbed the similarity score is near 1. However, when high variance components are perturbed the angular Procrustes score drops much more than for CKA and Normalized Bures Similarity (NBS). (b, c) We jointly optimized the values of both angular Procrustes and CKA or linear regression to illustrate the allowed ranges of both similarity scores (gray region enclosed by the solid lines). The pink dots in panel c indicate the target values for optimization, and the blue curves indicate the optimization trajectories of the two similarity measures. If angular Procrustes has a high score of 0.9 (horizontal dashed line) then linear regression will have a value above this. In contrast, a high linear regression score of 0.9 (vertical dashed line) does not imply a high angular Procrustes score, and a wide range of angular Procrustes scores are possible.

details):

$$\text{CKA}(X, Y) = \frac{\|X^T Y\|_F^2}{\|X X^T\|_F \|Y Y^T\|_F} \quad \text{NBS}(X, Y) = \frac{\|X^T Y\|_*}{\sqrt{\|X X^T\|_* \|Y Y^T\|_*}}$$

NBS quantifies similarity using the nuclear norm, which involves a sum of singular values, whereas CKA uses the Frobenious norm, which sums the square of the singular values. The additional square operation in CKA significantly increases the contribution of large variance components. We show this in theory by considering how CKA and NBS change when perturbing a single principal component of the data. The result is that CKA depends quadratically on the variance of the perturbed principal component, whereas NBS has a linear dependence (see proof in appendix B.3), as empirically validated in Figure 6a.

$$\text{CKA}(X, \tilde{X}_k) \approx \frac{\sum_{i \neq k} (\lambda_X^i)^2}{\sum_i (\lambda_X^i)^2} \quad \text{NBS}(X, \tilde{X}_k) \approx \frac{\sum_{i \neq k} \lambda_X^i}{\sum_i \lambda_X^i}$$

where \tilde{X}_k is equal to X where only the k^{th} principal component is modified.

4.4 Are metrics mutually independent?

A natural question that arises is whether these different similarity metrics are independent of each other, or if they exhibit consistent relationships. To address this, we consider three possible relationships between any two given similarity metrics (Figure 6b):

- **Independent:** The two metrics are independent. A high score on one metric offers no guarantee of a high score on the other.
- **Coupled:** The two metrics are tightly coupled. A high score on one metric implies a high score on the other, and vice versa.
- **Asymmetric:** One metric subsumes the other. A high score on the first metric guarantees a high score on the second, but not the other way around.

We jointly optimize multiple similarity scores to find their allowed ranges (Figure 6c) and show that a **high angular Procrustes similarity implies a high CKA score, but not the converse**. A high value of angular Procrustes implies a high score for unregularized linear regression but linear regression that is regularized and cross-validated across experimental conditions can take independent values.

5 Discussion

Our study reveals critical limitations of commonly used similarity measures for comparing models and neural datasets. While these measures offer a seemingly straightforward way to quantify

representational alignment, our optimization-based approach shows that high similarity scores, particularly for CKA and linear regression, do not guarantee that synthetic datasets encode task-relevant information in a manner consistent with neural data. Specifically, we demonstrate that measures like CKA are heavily influenced by the top principal components of the data, often achieving high scores even when lower variance components, which might carry crucial task-related information, remain poorly captured.

Limitations & future work. Our study focused on differentiable, geometry-based similarity measures and their optimization dynamics. Future work should investigate how it extends to other types of measures. Additionally, a comprehensive analysis of computational efficiency and scalability for different metrics will be crucial as datasets continue to grow in size. Moving forward, our python package aims to standardize similarity measures, facilitating a more cumulative scientific approach by centralizing findings related to these measures, and enabling more integrated benchmarking and comparisons.

References

- Nathan Cloos, Moufan Li, Guangyu Robert Yang, and Christopher J. Cueva. Scaling up the evaluation of recurrent neural network models for cognitive neuroscience. *Conference on Cognitive Computational Neuroscience (CCN)*, 2022.
- Frances Ding, Jean-Stanislas Denain, and Jacob Steinhardt. Grounding representation similarity through statistical testing. In *Advances in Neural Information Processing Systems*, volume 34, 2021.
- Jeremy Freeman, Corey M Ziemba, David J Heeger, Eero P Simoncelli, and J Anthony Movshon. A functional and perceptual signature of the second visual area in primates. *Nature Neuroscience*, 16(7):974–981, July 2013. ISSN 1546-1726.
- Sarah E Harvey, Brett W. Larsen, and Alex H Williams. Duality of bures and shape distances with implications for comparing neural representations. In *UniReps: the First Workshop on Unifying Representations in Neural Models*, 2023.
- Nicholas G. Hatsopoulos, Qingqing Xu, and Yali Amit. Encoding of movement fragments in the motor cortex. *Journal of Neuroscience*, 27(19):5105–5114, 2007.
- Sepp Hochreiter and Jürgen Schmidhuber. Long short-term memory. *Neural computation*, 9:1735–80, 12 1997.
- Diederik P. Kingma and Jimmy Ba. Adam: A method for stochastic optimization, 2017.
- Max Klabunde, Tobias Schumacher, Markus Strohmaier, and Florian Lemmerich. Similarity of neural network models: A survey of functional and representational measures, 2023.
- Simon Kornblith, Mohammad Norouzi, Honglak Lee, and Geoffrey Hinton. Similarity of neural network representations revisited, 2019.
- Nikolaus Kriegeskorte, Marieke Mur, Douglas A. Ruff, Roozbeh Kiani, Jerzy Bodurka, Hossein Esteky, Keiji Tanaka, and Peter A. Bandettini. Matching categorical object representations in inferior temporal cortex of man and monkey. *Neuron*, 60(6):1126–1141, 12 2008.
- Richard D. Lange, Devin Kwok, Jordan Matelsky, Xinyue Wang, David S. Rolnick, and Konrad P. Kording. Neural networks as paths through the space of representations, 2022.
- Najib J. Majaj, Ha Hong, Ethan A. Solomon, and James J. DiCarlo. Simple learned weighted sums of inferior temporal neuronal firing rates accurately predict human core object recognition performance. *Journal of Neuroscience*, 35(39):13402–13418, 2015. doi: 10.1523/JNEUROSCI.5181-14.2015.
- Valerio Mante, David Sussillo, Krishna V. Shenoy, and William T. Newsome. Context-dependent computation by recurrent dynamics in prefrontal cortex. *Nature*, 503:78–84, Nov 2013.
- Kenneth D. Miller and Francesco Fumarola. Mathematical equivalence of two common forms of firing rate models of neural networks. *Neural Computation*, 24(1):25–31, 2012.
- Aran Nayebi, Daniel Bear, Jonas Kubilius, Kohitij Kar, Surya Ganguli, David Sussillo, James J DiCarlo, and Daniel L Yamins. Task-driven convolutional recurrent models of the visual system. *Advances in neural information processing systems*, 31, 2018.
- Martin Schrimpf, Jonas Kubilius, Ha Hong, Najib J. Majaj, Rishi Rajalingham, Elias B. Issa, Kohitij Kar, Pouya Bashivan, Jonathan Prescott-Roy, Franziska Geiger, Kailyn Schmidt, Daniel L. K. Yamins, and James J. DiCarlo. Brain-score: Which artificial neural network for object recognition is most brain-like? *bioRxiv preprint*, 2018.
- Martin Schrimpf, Jonas Kubilius, Michael J Lee, N Apurva Ratan Murty, Robert Ajemian, and James J DiCarlo. Integrative benchmarking to advance neurally mechanistic models of human intelligence. *Neuron*, 2020. URL [https://www.cell.com/neuron/fulltext/S0896-6273\(20\)30605-X](https://www.cell.com/neuron/fulltext/S0896-6273(20)30605-X).
- Markus Siegel, Timothy J. Buschman, and Earl K. Miller. Cortical information flow during flexible sensorimotor decisions. *Science*, 348(6241):1352–1355, 2015. doi: 10.1126/science.aab0551.

- Ilia Sucholutsky, Lukas Muttenthaler, Adrian Weller, Andi Peng, Andreea Bobu, Been Kim, Bradley C. Love, Erin Grant, Iris Groen, Jascha Achterberg, Joshua B. Tenenbaum, Katherine M. Collins, Katherine L. Hermann, Kerem Oktar, Klaus Greff, Martin N. Hebart, Nori Jacoby, Qiuyi Zhang, Raja Marjieh, Robert Geirhos, Sherol Chen, Simon Kornblith, Sunayana Rane, Talia Konkle, Thomas P. O’Connell, Thomas Unterthiner, Andrew K. Lampinen, Klaus-Robert Müller, Mariya Toneva, and Thomas L. Griffiths. Getting aligned on representational alignment, 2023.
- David Sussillo, Mark M Churchland, Matthew T Kaufman, and Krishna V Shenoy. A neural network that finds a naturalistic solution for the production of muscle activity. *Nature neuroscience*, 18(7): 1025–1033, Jul 2015.
- Shuai Tang, Wesley J. Maddox, Charlie Dickens, Tom Diethe, and Andreas Damianou. Similarity of neural networks with gradients, 2020.
- Alex H. Williams, Erin Kunz, Simon Kornblith, and Scott W. Linderman. Generalized shape metrics on neural representations. In *Advances in Neural Information Processing Systems*, volume 34, 2021.
- Daniel L. K. Yamins, Ha Hong, Charles F. Cadieu, Ethan A. Solomon, Darren Seibert, and James J. DiCarlo. Performance-optimized hierarchical models predict neural responses in higher visual cortex. *Proceedings of the National Academy of Sciences*, 111(23):8619–8624, 2014. doi: 10.1073/pnas.1403112111.

A Neural Datasets and Models

A.1 Datasets

We analyzed neural data from five studies on nonhuman primates:

- [Mante et al. \[2013\]](#): Prefrontal cortex (PFC) electrode recordings during a contextual decision-making task involving colored moving dots. [Data link](#)¹.
- [Siegel et al. \[2015\]](#): Frontal Eye Field (FEF) electrode recordings during a contextual decision-making task involving colored moving dots, similar to Mante et al. (2013).
- [Hatsopoulos et al. \[2007\]](#): Primary motor (M1) electrode recordings during a center-out reaching task. [Data link](#)².
- [Majaj et al. \[2015\]](#): Inferior temporal (IT) electrode recordings during object image presentations.
- [Freeman et al. \[2013\]](#): Primary (V1) and secondary (V2) visual area electrode recordings during texture and noise image presentations.

We use the BrainScore³ library [[Schrimpf et al., 2020](#)] for the [Majaj et al. \[2015\]](#), [Freeman et al. \[2013\]](#) datasets.

A.2 Recurrent Neural Network (RNN) models

We show results for three commonly used RNN architectures: LSTMs [[Hochreiter and Schmidhuber, 1997](#)] and two choices for continuous time recurrent neural networks (CTRNNs), which differ by the position of the nonlinearity [[Miller and Fumarola, 2012](#)]. A first alternative is given by the following equations.

$$\begin{cases} \tau \frac{dh}{dt} = -h + Wr + Bu + b \\ r = f(h) + \xi \end{cases}$$

where u is the input, h represents the membrane potential, ξ is a Gaussian white noise, and r is the firing rate produced by the model and is used to compare the model with the neural data. The second alternative is given by the following equation.

$$\tau \frac{dr}{dt} = -r + f(Wr + Bu + b) + \xi$$

We call it the LowPassCTRNN since it can be shown that its firing rate is a low-pass filter of the firing rate of the first architecture, which we call CTRNN [[Miller and Fumarola, 2012](#)]. The RNNs are trained using supervised learning on simplified task inputs and outputs.

A.3 Condition average baseline:

The condition average baseline is obtained by averaging the neural activity along the condition dimension, while still allowing each neuron to have its own unique time-varying firing rate, and then comparing this condition-averaged dataset to the original neural data. This baseline shows the similarity one can obtain by discarding the condition specific activity to keep only the condition independent dynamics of the neural activity.

B Similarity Measures

B.1 Definitions

Several methods have been proposed to measure similarity between models and neural data (see [[Sucholutsky et al., 2023](#)], [[Klabunde et al., 2023](#)] for comprehensive reviews). While some efforts

¹<https://www.ini.uzh.ch/en/research/groups/mante/data.html>

²<https://datadryad.org/stash/dataset/doi:10.5061/dryad.xsj3tx9cm>

³<https://github.com/brain-score/vision>

have been made to characterize these metrics mathematically, for instance, by examining their invariance properties, clear guidance on selecting the most appropriate metric for a given scenario remains limited. To address this gap, we introduce a novel method for analyzing the specific aspects of data prioritized by different similarity metrics. Our method leverages the differentiability of these metrics and is applicable to a wide range of measures. We focus here on three commonly used metrics and their variants, linear regression [Yamins et al., 2014, Schrimpf et al., 2018], Centered Kernel Alignment (CKA) [Kornblith et al., 2019], and Procrustes distance [Williams et al., 2021, Ding et al., 2021]. These methods quantify similarity based on the goodness of fit after aligning the representations. This alignment transformation allows for greater flexibility by making similarity measures invariant to specific transformations. For example, instead of demanding a one-to-one mapping of neurons between datasets, these methods can accommodate scenarios where neurons in one dataset correspond to linear combinations of neurons in the other.

Consider two datasets X and Y with shape (sample, feature) and mean-centered columns. Datasets with dynamics are shaped from (time, sample, feature) to (time*sample, feature).

Assuming X as our reference dataset (e.g., neural data), linear regression seeks the optimal linear mapping B to predict X from Y . We use the R^2 coefficient to evaluate goodness of fit and ridge regularization with parameter $\lambda = 100$, as well as 5-fold cross-validation. Note that we apply cross-validation after reshaping the data from (time, sample, feature) to (time*sample, feature).

$$R_{LR}^2 = 1 - \frac{\min_B \|X - YB\|_F^2 + \lambda \|B\|_F}{\|X\|_F^2}$$

It’s important to note that this score is not symmetric. Applying linear regression on Y, X instead of X, Y may yield significantly different scores. This asymmetry arises because one dataset might be highly predictive of the other, while the reverse might not hold true.

Unlike linear regression, CKA and Procrustes are symmetric, meaning the metric yields the same result whether applied to X, Y or Y, X . Moreover, they exhibit a different class of invariance. While linear regression is invariant under invertible linear transformations, CKA and Procrustes are invariant under orthogonal linear transformations. This stricter invariance to orthogonal transformations potentially reduces sensitivity to noise [Kornblith et al., 2019].

CKA measures the correlation between the kernels of two datasets X and Y [Kornblith et al., 2019]. We consider here linear CKA where the kernels are XX^T and YY^T .

$$\text{CKA}(X, Y) = \frac{\langle \text{vec}(XX^T), \text{vec}(YY^T) \rangle}{\|XX^T\|_F \|YY^T\|_F} = \frac{\|X^T Y\|_F^2}{\|XX^T\|_F \|YY^T\|_F}$$

CKA scores range from 0 to 1, with 1 indicating perfect similarity. We also consider the arccosine of CKA, a metric satisfying the axioms of a distance metric (e.g., the triangle inequality) with 0 signifying perfect similarity [Williams et al., 2021]. This metric, also known as Angular CKA [Lange et al., 2022], is then normalized to a similarity score between 0 and 1 for direct comparison with other scoring methods. This normalization involves dividing the angular distance by $\pi/2$ and subtracting the result from 1, ensuring the measure increases with similarity.

$$\text{AngularCKAScore}(X, Y) := 1 - \frac{\arccos(\text{CKA}(X, Y))}{\pi/2}$$

Procrustes distance provides another approach for quantifying similarity [Williams et al., 2021, Ding et al., 2021]. This metric identifies the optimal orthogonal alignment to maximize the correlation between X and Y :

$$\max_{Q \in \mathcal{O}} \frac{\langle X, QY \rangle}{\|X\|_F \|Y\|_F}$$

where \mathcal{O} is the group of orthogonal linear transformations. An angular distance metric can be obtained by taking the arccosine of this quantity.

As shown in Harvey et al. [2023], Procrustes distance is closely related to Normalized Bures Similarity (NBS) [Tang et al., 2020], with Procrustes distance equating the arccosine of NBS. NBS is defined as:

$$\text{NBS}(X, Y) = \frac{\|X^T Y\|_*}{\sqrt{\|XX^T\|_* \|YY^T\|_*}}$$

This definition resembles CKA but utilizes the nuclear matrix norm instead of the Frobenius matrix norm. The Frobenius norm, denoted by $\|A\|_F$ for a matrix A , is calculated as the square root of the sum of squared singular values. The nuclear norm, $\|A\|_*$, is simply the sum of singular values. The implications of this difference in matrix norms for the weighting of principal components by CKA and NBS are further explored in B.3.

Similar to the score version of CKA distance, we define a score version of Procrustes distance, ranging from 0 to 1, where 1 represents perfect similarity.

$$\text{AngularProcrustesScore}(X, Y) := 1 - \frac{\arccos(\text{NBS}(X, Y))}{\pi/2}$$

B.2 Optimizing similarity scores

To better characterize similarity measures we optimize synthetic datasets Y to become more similar to a reference dataset X . We initialize the synthetic dataset Y by randomly sampling from a standard Gaussian distribution with the same shape as X . We use Adam [Kingma and Ba, 2017] to optimize Y to maximize the similarity score with X , leveraging the differentiability of the similarity measures, and stop the optimization when the score reaches a fixed threshold.

As we optimize Y towards greater similarity with X , we simultaneously evaluate how well task-relevant variables can be linearly decoded from the evolving synthetic data. This decoding analysis employs logistic regression with stratified 5-folds cross-validation. For dataset with temporal dynamics, we fit a separate decoder for each time step and report the average accuracy across time.

We also evaluate how each principal component (PC) of the reference dataset X is captured as Y is optimized for similarity. Specifically, for each PC v_i of X , we use linear regression to find the optimal linear combination of columns of Y that best predicts v_i . The goodness of fit is then quantified using the R^2 coefficient:

$$R_{PC_i}^2 := 1 - \frac{\|(X - \hat{X})v_i\|^2}{\|Xv_i\|^2}$$

where $\hat{X} = Y\hat{B}$ and $\hat{B} = \text{argmin}_B \|X - YB\|_F^2$.

All experiments were conducted on a NVIDIA GeForce GTX TITAN X and required less than a day of compute time.

B.3 Proof: theoretical analysis of CKA and NBS

Our results show that similarity in the high variance components seem to dominate the Centered Kernel Alignment (CKA) score. In contrast metrics like Normalized Bures Distance (NBS) seem to be more sensitive to changes in lower variance components. We explain this difference by showing, in theory, how CKA and NBS changes when perturbing a single principal component of the data. The result is that CKA depends quadratically on the variance of the perturbed principal component, whereas NBS has a linear dependence. We start the derivation from the matrix norm definitions of CKA and NBS.

$$\text{NBS}(X, Y) = \frac{\|X^T Y\|_*}{\sqrt{\|X X^T\|_* \|Y Y^T\|_*}}$$

$$\text{CKA}(X, Y) = \frac{\|X^T Y\|_F^2}{\|X X^T\|_F \|Y Y^T\|_F}$$

Let X be a dataset, and Y be a perturbed version of X , denoted \tilde{X}_k , where only the k^{th} principal component is modified. Specifically, define Y such that its j^{th} left singular vector u_Y^j is equal to the j^{th} left singular vector u_X^j of X for all $j \neq k$, and define u_Y^k to be a perturbation of u_X^k that preserves variance. Here we randomly sample u_Y^k from a Gaussian distribution with the same variance as the variance of u_X^k so that $\sigma_Y^k = \sigma_X^k$. The right singular vectors of Y are the same as the right singular vectors of X . Intuitively this perturbation affects only the projection of the data along the k^{th} principal component.

We first show how $\text{CKA}(X, \tilde{X}_k)$ depends on the variance of the perturbed principal component. As shown in [Kornblith et al., 2019], CKA can be rewritten in terms of dot products of the left singular vectors.

$$\text{CKA}(X, Y) = \frac{\sum_{i,j} \lambda_X^i \lambda_Y^j \langle u_X^i, u_Y^j \rangle^2}{\sqrt{\sum_i (\lambda_X^i)^2} \sqrt{\sum_j (\lambda_Y^j)^2}}$$

where $X = U_X \Sigma_X V_X^T$, $Y = U_Y \Sigma_Y V_Y^T$ are the SVD decompositions of X and Y respectively, and $\lambda_X^i = (\sigma_X^i)^2$, $\lambda_Y^j = (\sigma_Y^j)^2$. Since $u_Y^j = u_X^j$ for all $j \neq k$ and since U_X is an orthogonal matrix, the dot products $\langle u_X^i, u_Y^j \rangle$ are equal to 0 for all $j \neq i$ whenever $j \neq k$. The dot products $\langle u_X^i, u_Y^k \rangle$ are not guaranteed to be zero since randomly sampling u_Y^k doesn't guarantee to preserve the orthogonality with the other left singular vectors. However, when the number of samples in the data is large the projection u_Y^k on the other singular vectors will be relatively small. With the assumption that $\langle u_X^i, u_Y^k \rangle \approx 0$, CKA can be written as:

$$\text{CKA}(X, \tilde{X}_k) \approx \frac{\sum_{i \neq k} (\lambda_X^i)^2}{\sum_i (\lambda_X^i)^2}$$

This shows that CKA scores between the original data and the perturbed data depend quadratically on the variance of the perturbed principal component. As shown in Figure 6, our theoretical approximation closely matches simulations.

As opposed to CKA, NBS cannot be directly rewritten as a sum of left singular vector dot products. However, we show that NBS reduces to a simple form when Y is defined as X perturbed along a single principal component and when $\langle u_X^i, u_Y^k \rangle \approx 0$ is assumed. We start by expressing the nuclear norm in the numerator of NBS in terms of the SVD decomposition of X and Y .

$$\|X^T Y\|_* = \|V_X \Sigma_X U_X^T U_Y \Sigma_Y V_Y^T\|_* = \|\Sigma_X U_X^T U_Y \Sigma_Y\|_*$$

The individual entries of the product of matrices inside the nuclear norm corresponds to the dot products between the left singular vectors of X and Y weighted by the corresponding singular values.

$$[\Sigma_X U_X^T U_Y \Sigma_Y]_{ij} = \sigma_X^i \sigma_Y^j \langle u_X^i, u_Y^j \rangle$$

By definition of $Y \equiv \tilde{X}_k$,

$$\sigma_X^i \sigma_Y^j \langle u_X^i, u_Y^j \rangle = \begin{cases} (\sigma_X^i)^2 \delta_{ij} & \text{if } j \neq k \\ \sigma_X^i \sigma_X^k \langle u_X^i, u_Y^k \rangle & \text{if } j = k \end{cases}$$

With our assumption that $\langle u_X^i, u_Y^k \rangle \approx 0$ and the nuclear norm property $\|A\|_* = \text{Tr}[\sqrt{A^T A}]$, we find:

$$\|X^T Y\|_* \approx \sum_{i \neq k} (\sigma_X^i)^2$$

Since our perturbation preserves the variance, we have $\|X X^T\|_* = \|Y Y^T\|_* = \sum_i (\sigma_X^i)^2$. We finally obtain the following approximation, which explicitly reveals the linear dependence of NBS on the variance of the principal components.

$$\text{NBS}(X, \tilde{X}_k) \approx \frac{\sum_{i \neq k} (\sigma_X^i)^2}{\sum_i (\sigma_X^i)^2} = \frac{\sum_{i \neq k} \lambda_X^i}{\sum_i \lambda_X^i}$$